Reducing uncertainty by integrating 3D CSEM in the Mexican deep-water exploration workflow

José Antonio Escalera Alcocer,[1] Marco Vázquez García,[1] and Humberto Salazar Soto,[1] Daniel Baltar,[2*] Valente Ricoy Paramo,[2] Pål T. Gabrielsen[2] and Friedrich Roth[2] show with four case studies how the inclusion of 3D CSEM resistivity data with seismic and other data provided more confidence in Pemex reservoir evaluations and so positively impacted the company`s exploration programme.

The addition of 3D CSEM derived resistivity to seismic data enables more certainty in the creation of a geologic model and provides higher confidence in the probability of success and reserve estimation evaluations.

To mitigate risk and prioritize an offshore exploration portfolio, it has become important for Pemex to adopt technologies that could improve prospect evaluation at a portfolio scale. After a pilot project in 2008, 3D controlled source electromagnetics (CSEM) was identified as one of these technologies. Between 2010 and 2012, Pemex acquired >12,000 km² of 3D CSEM over 35 prospects identified by 3D seismic data (see Figure 1). After drilling a number of these prospects, Pemex has found that integrating 3D CSEM data in its exploration workflow significantly reduced uncertainties in the evaluation of prospects and play types.

Building on the work of previous authors (Eidesmo et al., 2002; Stefatos et al., 2009; Fanavoll et al., 2010; Ridyard et al., 2011) this work focuses on the use and integration of 3D CSEM with other geophysical datasets to quantify and reduce exploration risk in four exploration cases subsequently validated by drilling results.

Statistical prospect evaluation

Prospects are usually evaluated based on three key parameters:
1. Probability of success
2. Minimum economic field size
3. Reserve estimation

The probability of success is the probability of finding a hydrocarbon accumulation that can sustain flow (Rose, 2001). In exploration settings the amount of available information is typically low; therefore the uncertainty on the probability assessment is high.

The minimum economic field size conveys engineering, geographical, and economic information and cannot usually be affected by the additional geophysical or geological information.

The reserve estimation typically suffers from such high uncertainties that it is statistical rather than deterministic. A recoverable reserve probability distribution is often generated using an equation similar to this:

$$RR = \frac{A \; \Delta Z \; \theta \; S_{HC} \; RF}{FVF}$$

Where RR are recoverable reserves, *A* is the area, ΔZ is the net reservoir thickness, θ is the porosity, S_{HC} is the hydrocarbon saturation, RF is the recovery factor and FVF is the hydrocarbon shrinkage factor. In an exploration scenario, the largest uncertainties are often in the area and net reservoir thickness.

The use and integration of 3D CSEM data in a statistical prospect evaluation reduces the uncertainty in the factors associated to probability of success and reserve estimation. This concept will be expanded in the next section.

Resistivity information from 3D CSEM

With scarce, distant, or not relevant well data, we typically rely on the structural images and elastic properties derived from seismic data and geologic analogues when evaluating an exploration project. Using the 3D seismic, we can evaluate the structure, seal (presence or absence), presence, and quality of the reservoir, fault patterns and then generate the surfaces for basin modelling. In some cases, seismic can be used to assess the presence of hydrocarbons in the reservoir and/or evaluate fluid migration.

The electrical resistivity of a sedimentary rock is largely determined by its porosity and the fluids occupying its pore space. A brine-saturated, good porosity reservoir rock will typically have low resistivity due to the low resistivity of brine. When hydrocarbon-filled, that same reservoir rock will become resistive. This concept has been the basis for the invention of resistivity logging in the 1920s and equally applies to CSEM. High formation resistivity, however, may also be a result of low porosity lithology, low pore space connectivity or very low salinity brine. Some hydrocarbon-filled

[1] PEMEX Subdirección de Exploración.
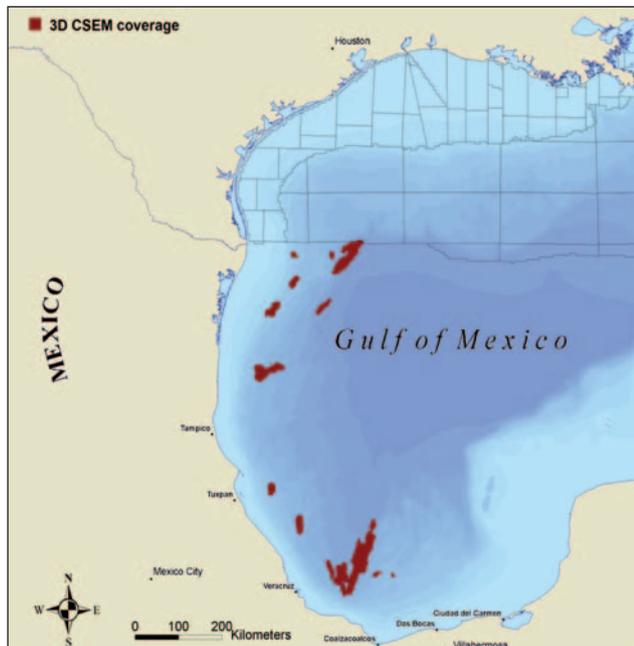[2] EMGS.
[*] Corresponding author, E-mail: dbaltar@emgs.com

Figure 1 Map showing where wide-azimuth 3D CESM has been acquired. Over 12,000 km2 were acquired over deep water prospects primarily defined using 3D seismic data.

reservoirs may exhibit low resistivity, a phenomenon commonly referred to as low-resistivity pay. The primary cause of low-resistivity pay is the presence of clay or conductive minerals. The various factors determining resistivity need to be carefully evaluated in a CSEM interpretation project.

Anisotropic inversion of 3D CSEM data provides an Earth model of vertical resistivity (Rv) and horizontal resistivity (Rh). The Rh volume is more sensitive to conductive layers and the Rv volume is more sensitive to resistive layers; thus Rv provides most of the information about the presence of hydrocarbons. The CSEM detectability of a thin resistive target mainly depends on the target area and transverse resistance (TR), or the product of target thickness x resistivity (vertical).

The absence of a resistive anomaly at the prospect location (negative CSEM response) could be due to factors that impact the probability of success such as the absence of hydrocarbons in the dataset or a low resistivity pay; or the reserve estimation, where hydrocarbons are present but the accumulation is too small (in terms of area, thickness, and saturation) to be detected. A resistivity anomaly (positive CSEM response), must be generated by a resistive body with enough area and thickness to be detected. There are several possible reasons for such a body to exist: high hydrocarbon saturation in the pore space, low porosity lithologies, or low connectivity pore space. For a positive or negative CSEM response, the likeliness of the interpretation must be assessed by integrating all the other available datasets, geological knowledge, and previous experience in the area. The quality, significance, and limitations of each dataset must be carefully assessed in order to generate a solid geologic model.

Integration of 3D CSEM resistivity

The integration of 3D CSEM with 3D seismic and geological information enhances the understanding of the subsurface by limiting the range of possible geological scenarios either by resolving an interpretation ambiguity or by reinforcing common, yet independent observations. This often translates to an improved understanding of the probability of success, and reserve estimation.

The following four case histories are integrated interpretations using 3D CSEM data with the aim of improving the prospect evaluation. In case A, a positive CSEM response example, there is a clear fit between the seismic and 3D CSEM data and therefore, the integrated interpretation has a high degree of certainty. For Cases B, C, and D, the seismic or CSEM data have quality limitations or the fit between both data sets is not clear; therefore, the evidence has to be carefully weighed resulting in a smaller uncertainty reduction in the interpretation.

Case A

The prospect is located approximately 700 m below mudline and is a classic anticlinal trap. The reservoir interval is a known regional interval and seismic attribute analysis confirms the regional geology at the prospect level. The petroleum system is proven and is not considered a major risk. The top of the reservoir interval presents a seismic bright spot with two associated flat spots, (Figure 2a and c) interpreted as gas-oil and oil-water contacts. This expected model is supported by the seismic amplitude analysis indicating the presence of a likely hydrocarbon-bearing reservoir. The main uncertainty is the hydrocarbon saturation; given the shallow depth to the reservoir, it is possible that low gas saturation is producing the bright amplitudes.

In the 3D CSEM inversion data, an Rv anomaly can be seen at the top of the structure and the resistivity anomaly is consistent with the uppermost part of the seismic anomaly and the first flat spot in the structure seen in Figure 2b.

After incorporating the 3D CSEM results, the integrated interpretation determined the accumulation consists of a good reservoir with high gas saturation down to the first flat spot and low hydrocarbon saturation further down dip. This observation provided an increase in the probability of success and a reduction in the reserve estimation for the prospect.

The interpretation was later confirmed by the drilling results from two wells. One well was inside the first flat spot encountering 40 m of net pay with high gas saturation and the second well, focused on a deeper target which has low CSEM sensitivity, encountered a similar reservoir interval in the down dip section but with low hydrocarbon saturation.

Case A illustrates the integration of 3D seismic and 3D CSEM data provides more interpretation certainty than using either dataset independently. Used separately, CSEM would have difficulty determining if the anomaly was hydrocarbon and seismic would have a high degree of uncertainty regarding the hydrocarbon saturation.
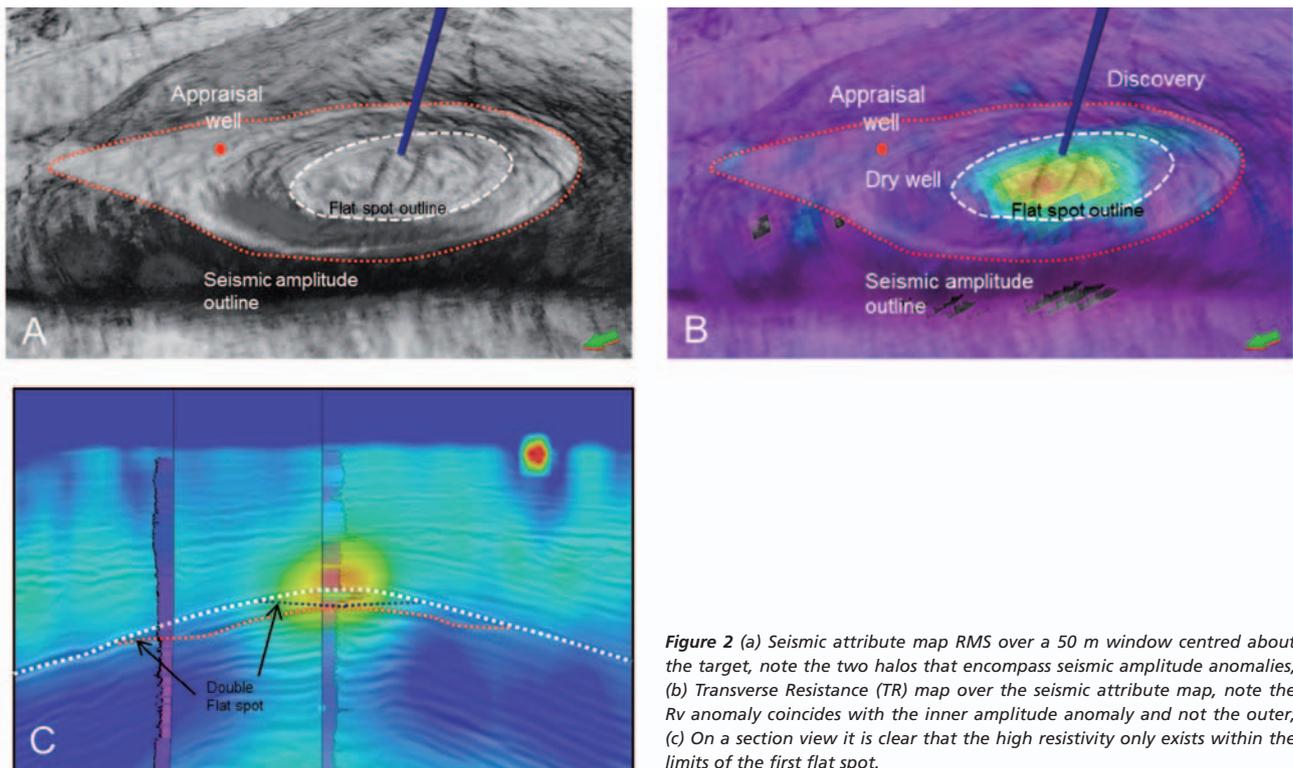
Figure 2 *(a) Seismic attribute map RMS over a 50 m window centred about the target, note the two halos that encompass seismic amplitude anomalies; (b) Transverse Resistance (TR) map over the seismic attribute map, note the Rv anomaly coincides with the inner amplitude anomaly and not the outer; (c) On a section view it is clear that the high resistivity only exists within the limits of the first flat spot.*

Case B

The prospect is approximately 2000 m below mudline and 175 km away from the nearest well providing direct geological information. The prospect is a classic anticline cored and pierced by a diapir interpreted to be clay dominated with remnants of salt. The reservoir interval has been defined through seismic attribute analysis, which allowed the interpretation and mapping of deep-water sand deposition. Seismic amplitude anomalies at the reservoir interval occur within a structural closure suggesting potential presence of a hydrocarbon-bearing reservoir. A series of normal faults above the crest of the structure are visible in the seismic and although these did not appear to reach the target objective, the faults extend vertically upwards to the seabed. Furthermore, at the seabed, circular escape features were noted with bright seismic events occurring just beneath. These observations suggest a relatively high seal integrity risk (Figure 3).

Wide-azimuth 3D CSEM data were acquired over the prospect and on close inspection, no Rv anomalies corresponded to the proposed target; instead, a low resistivity zone over the crest of the structure is present. This zone suggests the presence of high salinity brine around the faulting (Figure 3) resulting in an increase in the seal risk and a decreased probability of success. This is a case of CSEM affecting the geological model, and the lack of a CSEM anomaly at the target level indicates that the higher end of the area and thickness distributions entering in the reserve estimation are unlikely to exist.

This integrated interpretation was confirmed by a well that only encountered gas shows with good quality reservoir sands at the target level. Furthermore, the CSEM resistivity estimation showed an excellent fit with the well log resistivity trends (see Figure 4).

Case C

The prospect is located approximately 1800 m below mudline and consists of an anticlinal structure situated within a compressional belt where a variety of compressional structures
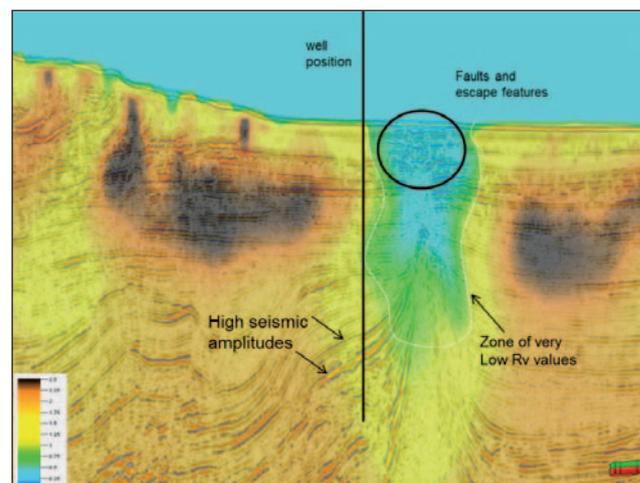

Figure 3 *Seismic section overlain with vertical resistivity (Rv) values from CSEM. Note the zone exhibiting very low Rv values and faulting below the seabed where an escape feature is indicated.*

occur at various scales. The prospect is riddled by faults displacing various stratigraphic levels including the interval where the target is located. Overlying the main structure, a seismic sequence is present which is almost devoid of faults, providing just enough sealing capacity for the entire structural closure.

The main target is a regional reservoir interval and it presents quite reasonable conformance with the structural closure and is associated with anomalous seismic amplitudes (Figure 5a). The initial interpretation relies purely on seismic data and geological knowledge and favours the presence of a
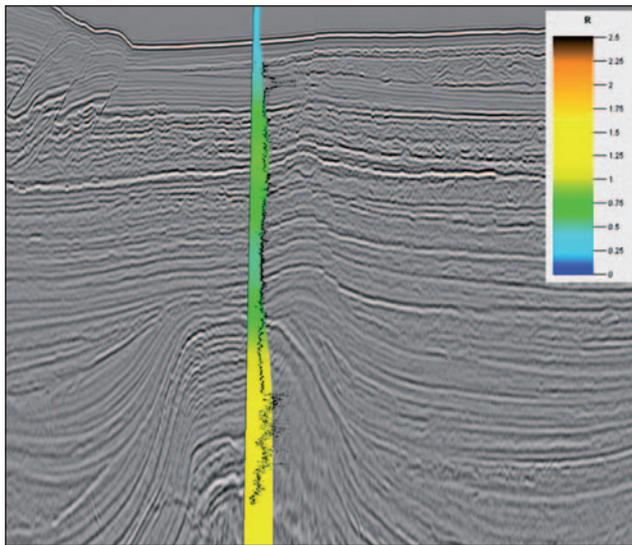

Figure 4 Seismic section along the structural closure. Well log resistivity (black line) is compared with the horizontal resistivity (Rh) estimated from CSEM; both are set at same scale.
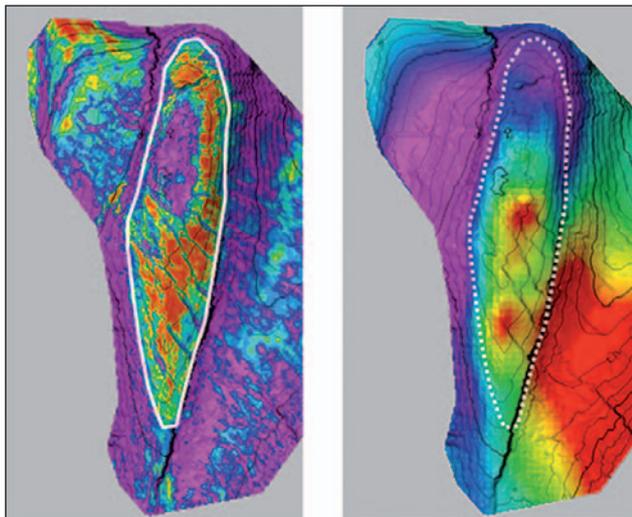

Figure 5 (a) RMS amplitude extraction map over the interval of interest; note the amplitude distribution and its conformance with structural closure. A white-line polygon shows the extent of the seismic anomaly. (b) A transverse resistance (TR) map showing the extent of the resistivity anomaly associated with the target. Note the close spatial correlation between both seismic and CSEM. The highly resistive feature to the SE of the main structure was interpreted as non-hydrocarbon related based on seismic indicators of resistive lithologies (not shown here).

hydrocarbon accumulation. The main risk is the hydrocarbon saturation/seal, as the column height is quite large.

In the 3D CSEM inversion data, an Rv anomaly is present that has a good fit with the seismic amplitudes within the structural closure (Figure 4b). This reduces the risk of low saturation being the origin of the seismic amplitudes, and confirms the large areal extent of the accumulation. With this interpretation, both the probability of success and reserves of this prospect were updated. The degree of uncertainty is higher in this case than the previous two cases as the seismic is affected by a shadow from shallow high amplitudes and the CSEM is affected by the presence of salt and a complicated overburden. There are other highly resistive features in the dataset, but they were interpreted as non-hydrocarbon related when integrated with the seismic data.

The target was drilled encountering two hydrocarbon-filled reservoir intervals and confirming the interpretation derived from the integration of regional geology, 3D seismic, and 3D CSEM data.

Case D

This prospect consists of a large anticline riddled with faults displacing various stratigraphic tiers and two known regional reservoir intervals 500 m and 1100 m below mudline. The shallow interval is characterized by strong seismic amplitudes with a large areal extent that indicate a high likelihood of a reservoir with risks in reservoir quality and hydrocarbon saturation. The deeper reservoir is shadowed by the high seismic amplitudes above, thus making a complete interpretation of the seismic amplitudes at the reservoir level challenging. Some bright amplitudes can be mapped inside and outside the shadowed area but the higher risk for this deeper target is reservoir distribution and hydrocarbon saturation.

The 3D CSEM data in the area are of very good quality and considered to have excellent sensitivity to both target levels. There is no resistivity associated to the first target implying an increased risk of low hydrocarbon saturation (lower probability of success) and a decrease in the expected reserves associated with this target. The second target has an Rv anomaly associated with it, and when mapped as TR, the resistivity anomaly is clearly limited by the main fault set that runs along the structural axis (Figure 6). Other smaller faults in the structure seem to act as TR boundaries, thus providing some insight into the hydrocarbon distribution inside the reservoir. These results allowed for a change in the evaluation of both targets: first target was deemed as low value, while the value of the second target can be increased significantly, mainly through a significant reduction in the reserve estimation uncertainty. The lack of supporting seismic amplitudes for the second objective reduces our ability to reduce its uncertainties further. The low seismic data quality makes the resistivity data more valuable as it provides an insight on the hydrocarbon-filled reservoir distribution that the seismic could not produce.
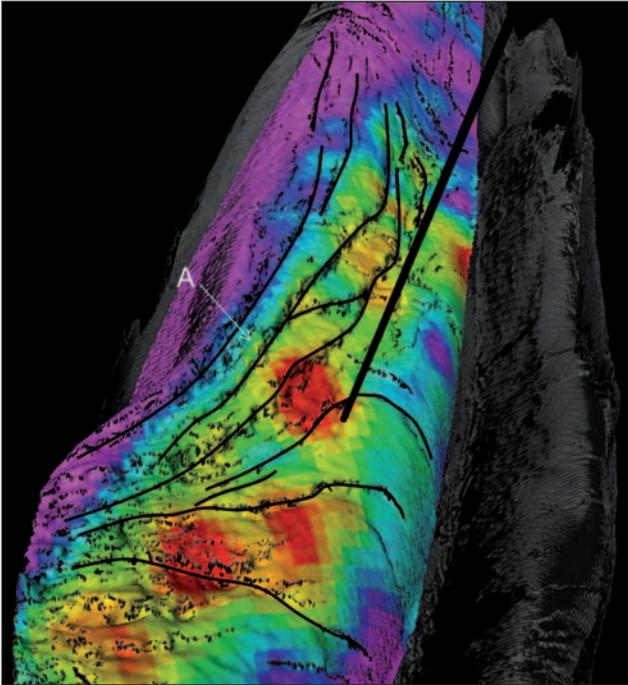
Figure 6 Co-visualization of transverse resistance (TR) overlain on a structural map at the target objective and seismic variance attribute. Note the fault layout with faults striking mainly N–S to NE–SW. There is good spatial correlation between the TR magnitudes and the fault layout in particular along the structural trend defined by fault A. Furthermore, there is spatial correlation between individual fault blocks and TR magnitudes suggesting compartmentalization.

A well was drilled encountering a low saturation reservoir in the shallow target and a hydrocarbon charged reservoir (approx. 60 m of net pay) at 1100 m below mudline. The well has been announced as a discovery, and the integration of both seismic-structural interpretations and the Rv anomaly distribution is used to enhance the understanding of hydrocarbon accumulation and distribution within this discovery.

Conclusions

- The addition of a new data set measuring an independent earth property, such as resistivity, should reduce interpretation uncertainty. By adding 3D CSEM to the workflow, we can reduce uncertainties associated with an incomplete geological model. Utilizing an improved geologic model during prospect evaluation results in a more accurate assessment of the probability of success, and reserve estimation.
- When a common interpretation is derived from independent datasets, interpretation uncertainty can be very low (Case A). When the quality, sensitivity or meaning of the data, seismic or CSEM, is compromised, e.g., due to complexity or limited sensitivity, uncertainty will be higher (Cases B, C, and D).
- The quality and assertiveness of each dataset must be carefully evaluated. It is extremely important that interpreters are capable of understanding the strengths and limitations

of each dataset to produce a sensible joint interpretation of all the data.
- Four case histories were used to illustrate the positive impact of using CSEM resistivity data in an integrated interpretation to improve prospect evaluation at a portfolio scale in accordance to probability of success and reserve estimation.

References

Eidesmo, T., Ellingsrud, S., MacGregor, L.M., Constable, S., Sinha, M.C., Johansen, S., Kong, F.N. and Westerdahl, H. (2002) Sea Bed Logging (SBL), a new method for remote and direct identification of hydrocarbon filled layers in deepwater areas. *First Break*, **20**(3), 144–152.

Fanavoll, S. et al. [2010] Controlled source electromagnetic technology and hydrocarbon exploration efficiency. *First Break*, **28**(5), 61–69.

Ridyard, D. and Hesthammer, J., (2011) Recent advances in controlled source EM have created new business opportunities by changing the risk equation in offshore exploration drilling. *World Oil*. March, 51–54.

Rose, P.R. [2001] *Risk analysis and management of petroleum exploration ventures*. AAPG Methods in Exploration Series, No. 12, p. 33.

Stefatos, A., Boulaenko, M. and Hesthammer, J. (2009) Marine CSEM technology performance in hydrocarbon exploration - limitations or opportunities? First Break. 27(5), 65-71.